Desalination and Water Treatment
www.deswater.com

26 (2011) 236–242
February

doi: 10/5004/dwt.2011.1543

Effect of gradually varying baffled-ring distance on ultrafiltration in tubular membranes inserted concentrically with a ring rod

Ho-Ming Yeh*, Cha-Hsing Li, Cha-Chun Lin

Department of Chemical and Materials Engineering, Tamkang University, Tamsui, Taipei county 251, Taiwan
Tel. +886 2 26215656; email: hmyeh@mail.tku.edu.tw

Received 2 October 2009; Accepted 10 August 2010

ABSTRACT

The decline of permeate flux along the membrane ultrafilters is mainly due to the increment in concentration polarization resistance and the decline of transmembrane pressure. It was found that the concentration polarization resistance could be reduced in a ring-rod tubular membrane ultrafilter by the turbulent behavior. The performance will be further improved if the baffled-ring distances gradually and properly decrease along the cross-flow channel with fixed number of baffled rings. Theoretical analysis was based on the mass and momentum balances coupled with the application of resistance-in-series model. Correlation predictions are rather acceptable for higher feed concentration comparing with the experimental results for ultrafiltration of dextran T500 aqueous solution in a tubular ceramic membrane of a nine-ring rod insert with gradually decreasing the baffled-ring distances.

Keywords: Ultrafiltration; Tubular membrane; Baffled-ring distance; Ring-rod insert

1. Introduction

The good fluid management at the membrane surface plays an important role in successful application of ultrafiltration. In almost all cross-flow ultrafiltration the permeate flux declines along the flow direction because of the concentration polarization and progressive fouling by the rejected particles [1,2]. Many hydraulic approaches, such as increasing fluid velocity or creating turbulent behavior, developed for reducing the concentration polarization resistance and progressive fouling to enhance the ultrafiltration flux, have been thoroughly discussed [3–14]. Actually, raising fluid velocity or creating turbulent behavior in the cross-flow membrane modules has two conflicting effects on ultrafiltration: They are the desirable effect of decrease in concentration polarization resistance and the undesirable effect of increase in frictional pressure loss. Since, along the flow channel in an ultrafilter, transmembrane pressure decreases while concentration polarization resistance increases. It appears therefore that gradually increasing the turbulent strength along the flow channel might suitably suppress the increasing resistance to permeation due to concentration polarization while properly maintaining the decreasing tranemembrane pressure. It is the purpose of present study to investigate the effect of varying baffled-ring distance on ultrafiltration and to derive the prediction equation for estimating the permeate flux, in a tubular membrane of a ring-rod insert with decreasing buffled-ring distance.

2. Analysis

Consider a tubular-membrane module of length L and radius r_m inserted concentrically with a solid rod of radius kr_m, wrapped with (N–1) baffled-ring of gradually decreasing ring distances d_j along the solid rod with arithemetic series of constant difference a, as shown in Fig. 1. Thus

*Corresponding author.

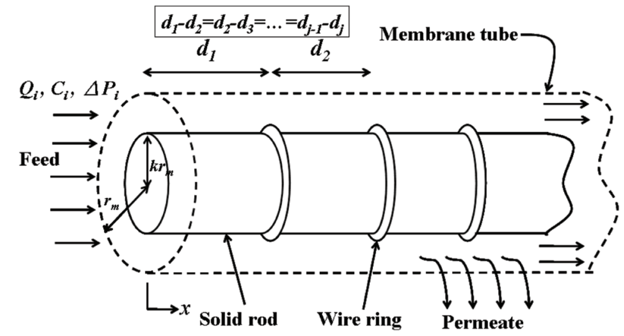

Fig. 1. Ring-rod membrane tube.

$$L = \sum_{j=1}^{N} d_j = \sum_{j=1}^{N} [d_1 - (j-1)a]\,, \quad j = 1, 2, 3, \cdots, N \tag{1}$$

2.1. Mass balance

Let $Q(z)$ be the volumetric flow rate of solution in a ring-rod membrane tube and $J(z)$ be the permeate flux by ultrafiltration. Then a mass balance over a slice dz of the flow channel gives

$$\frac{dQ}{dz} = -2\pi\, r_m \bar{J} \tag{2}$$

Since the permeation rate of membrane ultrafiltration is much smaller than the volume flow rate, J in Eq. (2) may be taken as its average value, i.e.,

$$\bar{J} = \frac{1}{L}\int_0^L J(z)\, dz \tag{3}$$

The declination behavior of volume flow rate along the tube is readily obtained by integrating Eq. (2) with the entrance condition: $Q = Q_i$ at $z = 0$, as

$$Q = Q_i - 2\pi\, r_m \bar{J} z \tag{4}$$

2.2. Momentum balance

As mentioned before, since the permeation rate of membrane ultrafiltration is small compared with the volume flow rate, it can be assumed that the rate of momentum transfer by convection may be neglected for momentum balance, i.e.,

$$\frac{d(\Delta P)}{dz}[\pi\, r_m^2(1-k^2)]dz + 2\pi\, r_m(\tau_1 + k\tau_2)dz = 0 \tag{5}$$

where $\Delta P = (P - P_s)$ denotes the transmembrane pressure, and $P(z)$ and P_s are the pressures in tube and shell sides, respectively, while τ_1 and τ_2 are the shear stresses on the membrane and ring-rod surfaces, respectively. Since the shear stress τ_1 is related to the friction factor $\bar{f}_1$ as

$$\tau_1 = \frac{\bar{f}_1 \rho\, u_b^2}{2} \tag{6}$$

and the bulk velocity of fluid in the flow channel is

$$u_b = \frac{Q}{\pi\, r_m^2(1-k^2)} \tag{7}$$

Thus, with the use of Eqs. (4) and (7), Eq. (6) becomes

$$\tau_1 = \frac{\bar{f}_1 \rho \left(Q_i - 2\pi\, r_m \bar{J} z\right)^2}{2\pi^2 r_m^4 \left(1-k^2\right)^2}$$

Finally, we have the momentum balance equation as

$$\frac{d(\Delta P)}{dz} + \frac{\bar{f} \rho\, (Q_i - 2\pi\, r_m \bar{J} z)^2}{\pi^2 r_m^5 (1-k^2)^3} = 0 \tag{8}$$

where $\bar{f}$ denotes the average friction factor defined by

$$\bar{f} = \bar{f}_1 + k\bar{f}_2 \tag{9}$$

2.3. Declination of transmembrane pressure

Integrating Eq. (8) from $z = 0$ ($\Delta P = \Delta P$) to $z = z$, one has the declination of transmembrane pressure along the flow channel as

$$\Delta P = \Delta P_i - A[1 - (1 - Bz)^3] \tag{10}$$

where

$$A = \frac{\bar{f}\ \rho\ Q_i^3}{6\pi^3 r_m^6 \bar{J} (1-k^2)^3} \tag{11}$$

$$B = \frac{2\pi\, r_m \bar{J}}{Q_i} \tag{12}$$

2.4. Permeate flux

The resistance-in-series model may be employed to express the permeate flux as [15]:

$$J(z) = \frac{\Delta P(z)}{R_m + R_f + \phi\, \Delta P(z)} \tag{13}$$

where R_m denotes the intrinsic resistance of membrane, R_f the resistance due to fouling phenomena, such as solute adsorption, while $\phi \Delta P(z)$ the resistance due to the concentration polarization/gel layer, which will be proportional to the amount and specific hydraulic resistance of the compressible layer deposited and may be assumed to be a linear function of transmembrane pressure with ϕ as a proportional constant.

The average value of permeate flux is readily obtained by substituting Eqs. (10) and (13) into Eq. (3)

$$\begin{aligned}\bar{J} &= \frac{1}{L}\int_0^L \frac{dz}{\phi[1+(C/\Delta P)]} = \frac{1}{L\phi}\int_0^L \left[1-\frac{C}{C+\Delta P}\right] dz \\ &= \frac{1}{\phi}\left[1-\frac{1}{L}\int_0^L \frac{C\,dz}{(C+\Delta P_i - A)+A(1-Bz)^3}\right]\end{aligned} \quad (14)$$

where

$$C = (R_m + R_f)/\phi \quad (15)$$

The integration of Eq. (14) was readily obtained but will not be presented here due to the long and cumbersome expression.

3. Experimental

3.1. Experimental value of $\bar{J}$

The experimental apparatus, materials and procedure were exactly the same as those in previous work [16], except that the wire spiral wrapped on the solid rod was replaced by nine ring baffles, having ring-wire diameter of 1 mm, as shown in Figs. 1 and 2. The membrane medium used in the ring-rod module was mainly a 150 kDa MWCO tubular ceramic membrane (M_2 type, Tech-sep, France; length L = 0.4 m, i.d. $2r_m$ = 6 mm) inserted concentrically with a baffled-ring rod of radius kr_m ($k = \frac{1}{2}$). The distance between two rings d_j at jth section decreases along the steel rod by arithemetic series with constant difference a, as

$$d_j = d_1 - (j-1)\mathrm{a}, \quad j = 1, 2, 3, \cdots, 10 \quad (16)$$

From Eq. (1) with N = 10 and L = 0.4 m

$$0.4 = \sum_{j=1}^{10} d_j = 10d_1 - 45\mathrm{a} \quad (17)$$

and

$$d_1 = 0.04 + 4.5\mathrm{a} \quad (18)$$

The solvent was distilled water. Many experimental results [17] for average permeate flux $\bar{J}$ were obtained, as well as the outlet transmembrane pressure ΔP_0 and solution volumetric flow rate Q_0 were measured, under various operating conditions: C_i = 0.1 and 0.5 wt%; $Q_i = 1.67\times10^{-6} - 4.17\times10^{-6}$ m^3/s; $\Delta P_i = 30-140$ kPa; k = 0 (without ring rod) and 1/2; a/L = 0 – 0.017. Some of the results of $\bar{J}$ are plotted in Figs. 3–6.

3.2. Correlation equations for R_m, R_f and ϕ

The values of ϕ and ($R_m + R_f$) were determined graphically from the experimental data of $(\bar{J})_{exp}$ and $(\Delta P)_{exp} = [(\Delta P_i + \Delta P_0)/2]_{exp}$ for various operating

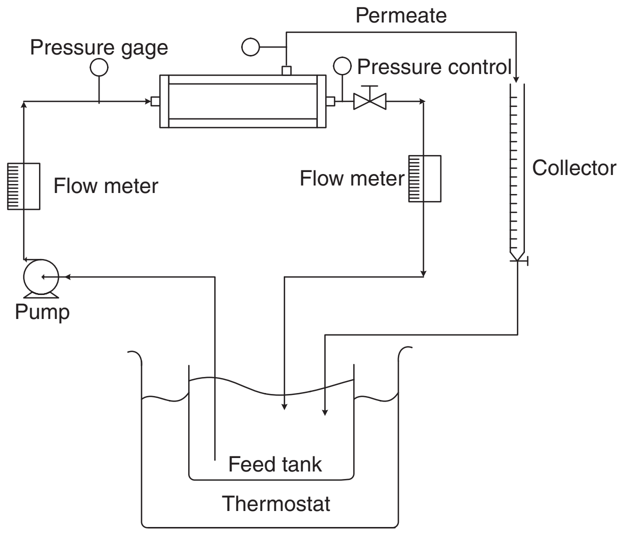

Fig. 2. Experimental apparatus.

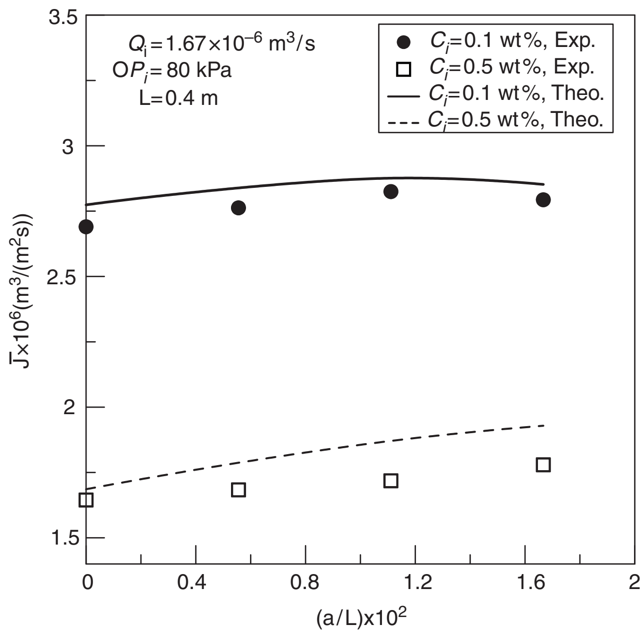

Fig. 3. Permeate flux vs. a/L for ΔP_i = 80 kPa and $Q_i = 1.67\times10^{-6}$ m^3/s.

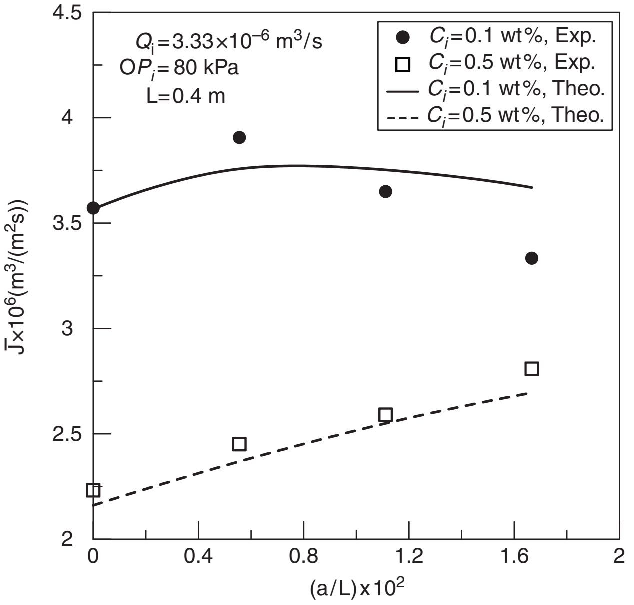

Fig. 4. Permeate flux vs. a/L for ΔP_i = 80 kPa and Q_i = 3.33 × 10^{-6} m^3/s.

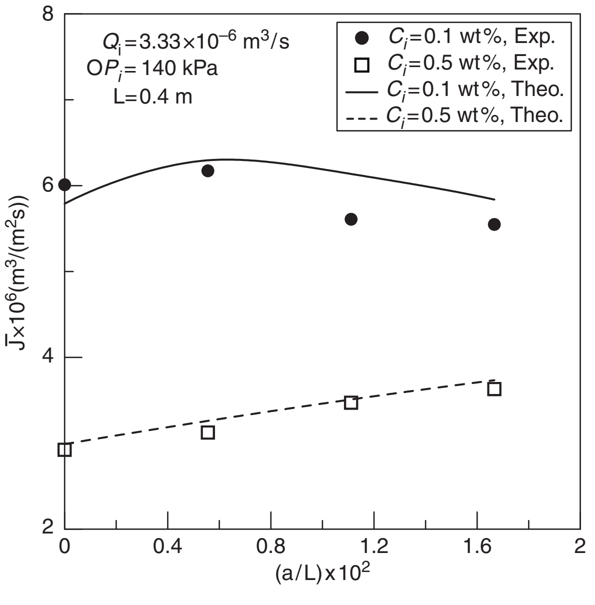

Fig. 5. Permeate flux vs. a/L for ΔP_i = 140 kPa and Q_i = 3.33 × 10^{-6} m^3/s.

conditions (C_i, ΔP_i and $u_i = Q_i/\pi\, r_m^2(1-k^2)$, by following the same procedures performed in previous works [13,14] with Eq. (13) modified as

$$\frac{1}{(\overline{J})_{\text{exp}}} = \phi + \frac{R_m + R_f}{(\overline{\Delta P})_{\text{exp}}} \qquad (19)$$

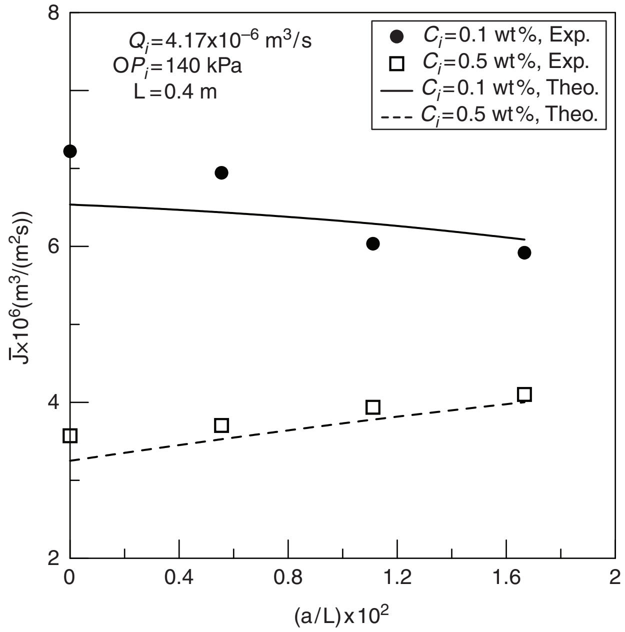

Fig. 6. Permeate flux vs. a/L for ΔP_i = 140 kPa and Q_i = 4.17 × 10^{-6} m^3/s.

With the use of the experimental data, it was found that a plot of $1/(\overline{J})_{\text{exp}}$ vs. $1/(\overline{\Delta P})_{\text{exp}}$ at certain u_i and C_i could be constructed as a straight line by the least squares method, and the values of ϕ (the intersection of ordinate) and (R_m + R_f) (the slope) were determined as functions of u_i, C_i and (a/L). It was observed from the experimental result that ϕ and R_f increase with C_i and decrease when u_i and (a/L) increase, while R_m is a constant (1.63 × 10^{10} Pa · s/m), for the membrane and test solution used in present study. Therefore, one may apply the power-law relations for constructing the correlation equations of these resistances with the independent experimental parameters.

Accordingly, the correlation equations for ϕ and ($R_m + R_f$) were constructed by the method of least squares method as function of u_i, C_i and a/(L/N) with L = 0.4 m and N = 10, i.e., [17]:

$$\phi = 2.02 \times 10^5 u_i^{-0.565} C_i^{1.38} [1 - (a/4) \times 10^2]^{1.082} \text{ s/m} \qquad (20)$$

$$R_m + R_f = 1.63 \times 10^{10} + 3.06 \times 10^9 u_i^{-0.644} C_i^{0.442} [1 - (a/4) \times 10^2]^{3.423} \text{ Pa} \cdot \text{s/m} \qquad (21)$$

3.3. Correlation equation for $\overline{f}$

The overall friction factor may be determined experimentally from Eq. (8) with the experimental values measured at the inlet (ΔPi, Q_i) and at the outlet (ΔP_0, Q_0), i.e.,

$$\frac{\Delta P_i - (\Delta P_0)_{\exp}}{L} = \frac{\bar{f}\rho\left[\frac{(Q_i + Q_0)_{\exp}}{2}\right]^2}{\pi^2 r_m^5 (1-k^2)^3} \tag{22}$$

or

$$\bar{f} = \frac{\pi^2 r_m^5 (1-k^2)^3 [\Delta P_i - (\Delta P_0)_{\exp}]}{L\rho\left[\frac{(Q_i + Q_0)_{\exp}}{2}\right]^2} \tag{23}$$

where the volumetric flow rate at the outlet is

$$Q_0 = Q_i - 2\pi\, r_m L \bar{J} \tag{24}$$

Many values of $\bar{f}$ were thus obtained with use of the experimental data [17]. The correlation equation for $\bar{f}$ was also constructed in the power-law relation by the method of least squares as functions of Reynolds number, Re, and the variation factor of ring distance, a/(L/N = a/0.04), i.e.,

$$\bar{f} = 2.27 \times 10^4 \mathrm{Re}^{-1.89} (1 - 0.25\mathrm{a} \times 10^2)^{-9.012} \tag{25}$$

where

$$Re = \rho \bar{u} D_e / \mu = (\rho/\mu)[(Q_i + Q_0)/\{2 r_m^2 \pi (1-k^2)\}][2(1-k) r_m] \tag{26}$$

in which $D_e = 2(1-k)r_m$, is the equivalent diameter of the concentric tube.

4. Results and discussion

4.1. Comparison of correlation predictions with experimental results

The average values of permeate flux $\bar{J}$ were calculated from Eq. (14) by iteration method coupled with the use of the correlation equations, Eqs. (20), (21) and (25), and some of the predicted values are compared with the experimental data, as shown in Figs. 3–6. It is seen in these figures that the correlation predictions are rather acceptable for higher feed concentration, while comparing with the experimental results. The average permeate flux increases with the inlet volumetric flow rate Q_i and transmembrane pressure ΔP_i, but decreases when the inlet concentration C_i increases.

4.2. Effect of a on $\phi\Delta P$

Since the thickness of concentration-polarization layer is small at the inlet and then increases along the flow channel, larger ring distance for less increment in turbulent behavior around the inlet region of a ring-baffle device is sufficiently enough to reduce the lower concentration-polarization resistance. In the meantime, smaller ring distance, as well as stronger turbulent behavior, around the outlet region is required for suppressing the higher concentration-polarization resistance. In present study, therefore, we are concerning with the device of gradually increasing the turbulent behavior along the flow channel by gradually decreasing the ring-baffle distance along the arithematic series of constant difference a, and with constant number N of total rings. Consequently, the concentration polarization resistance, $\phi\Delta P$, decreases when the ring-baffle distance decreases more rapidly, especially for higher feed concentration, as shown in Table 1.

4.3. Effect of a on $\bar{J}$

The increase in turbulent strength by gradually decreasing the baffle-ring distance actually has two conflict effects on permeate flux. One, the decreases in resistance to permeation due to reduction in concentration polarization, is good for ultrafiltration, while the other, the increases in pressure drop, as well as the decreases

Table 1
Experimental results of permeate flux and concentration polarization resistance for C_i = 0.5 wt.%

$Q_i \times 10^6$	$\Delta P_i \times 10^{-5}$	$\bar{J}_0 \times 10^6$	d_1 = 0.05 m and a = (0.02/9) m			d_1=0.06 m and a = (0.04/9) m			d_1 = 0.07 m and a = (0.06/9) m		
(m³/s)	(Pa)		$(\bar{J}) \times 10^6$ (m/s)	I (%)	$\phi\,(\overline{\Delta P}) \times 10^{-10}$ (Pa · s/m)	$(\bar{J}) \times 10^6$ (m/s)	I (%)	$\phi\,(\Delta P) \times 10^{-10}$ (Pa · s/m)	$(\bar{J}) \times 10^6$ (m/s)	I (%)	$\phi\,(\overline{\Delta P}) \times 10^{-10}$ (Pa · s/m)
1.67	0.3	0.7363	0.9670	31.34	1.020	0.9980	35.54	1.006	1.0120	37.45	0.983
	1.4	1.7544	2.0746	18.25	4.761	2.1000	19.70	4.694	2.2020	25.54	4.585
4.17	0.3	0.8025	1.2195	51.96	0.349	1.2407	54.60	0.289	1.2658	57.73	0.286
	1.4	2.3923	3.7035	54.81	1.630	3.9368	64.56	1.347	4.1016	71.45	1.336

in transmembrane pressure, due to increases in friction loss, is bad for ultrafiltration. It appears, therefore, that proper adjustment of turbulent strength along the flow channel as well as proper arrangement of the baffle-ring distance with a specified operating conditions (C_i, Q_i and ΔP_i), might effectively suppress any undesirable resistance to permeation due to concentration polarization while still preserving an effective transmembrane pressure, and thereby lead to improved permeate recoveries.

It is seen in Figs. 3–6 that for higher feed concentration (say C_i = 0.5 wt%), permeate flux increases when the baffle-ring distance gradually decreases more rapidly along the flow channel, as well as when the constant difference of arithemetic series, a, increases. This is because that the concentration polarization layer is thicker when the feed concentration is higher and thus, stronger turbulent is need to reduce the permeation resistance. For lower feed concentration, however, the concentration resistance is smaller and only moderate strength of turbulent behavior is sufficient enough to reduce the concentration polarization resistance, while still preserving the effective transmembrane pressure. Accordingly, for specified operating conditions (C_i, Q_i, ΔP_i), there may exsit an optimal value of a for maximum permeate flux, especially for lower feed concentration with larger volumetric flow rate, as shown in Figs. 3–6 for C_i = 0.1 wt%.

4.4. Improvement in performance

The improvement in performance resulting from operating a tubular membrane inserted concentrically with a ring rod is best illustrated by calculating the percentage increases in permeate flux based on the tubular membrane without a ring rod ($k = 0, \bar{J} = \bar{J}_0$)

$$I = \frac{\bar{J} - \bar{J}_0}{\bar{J}_0}$$

Some results for C_i = 0.5 wt% are shown in Table 1. Considerable improvement in permeate flux is obtainable by employing a baffle-ring tubular membrane with constant ring number N and with ring distances dj decreasing gradually along the ultrafilter. It is seen in Table 1 that 71.45% improvement is achieved when a = (0.06/9) m.

4.5. Energy expended

Although inserting such baffled-ring rod assembly can enhance permeate flux, the increase in hydraulic dissipated powers should be also taken into consideration. Nevertheless, the hydraulic dissipated powers W in such modules are small and the increase in operating cost may be ignored. Let us take the critical case (C_i = 0.5 wt%, $Q_i = 4.17\times10^{-6}$ m^3/s, k = 1/2, a = (0.06/9) m, $\Delta P_i = 1.4\times10^5$ Pa and $\Delta P_0 = 1.36\times10^5$ Pa)) shown in Table 1, as well as in [17], as example:

$$\begin{aligned} W &= (\rho Q_i)\frac{\Delta P_i - \Delta P_o}{\rho} = Q_i(\Delta P_i - \Delta P_o) \\ &= 4.17\times10^{-6}(1.4 - 1.36)\times10^5 \\ &= 1.668\times10^{-2}\ \mathrm{Nm/s} = 2.24\times10^{-5}\,\mathrm{hp} \end{aligned}$$

5. Conclusion

Ultrafiltration in a tubular membrane with decreasing baffled-ring distance of a ring-rod insert, has been investigated both theoretically and experimentally. The baffled-ring membrane module is modified from a tubular-membrane by inserting concentrically a steel rod wrapped with N-baffled rings of gradually decreasing ring distance along the module. Theoretical analysis was based on the mass and momentum balances coupled with the application of resistance-in-series model. Ultrafiltration of an aqueous solution of dextran T500 in the baffled-ring membrane tube of 0.4 m length (L), having the diameters of tube (r_m = 0.006 m), rod (kr_m = 0.003 m) and ring wire (0.001 m), was carried out for various transmembrane pressures (ΔP_i), feed concentrations (C_i), feed flow rates (Q_i) and ring distances (d_j). The total number of rings were fixed at nine (i.e., N = 10) and their distances decreased gradually along the module, as indicated by Eqs. (16) and (18). The comparison of the correlation predictions with experimental results are rather acceptable for higher feed concentration. Ultrafiltration in the module without ring rod (k = 0) was also carried out and with the results, the improvement in performance by inserting the ring rod was proved. This is because that by applying the ring-rod device, the desirable effect of reducing the concentration polarization resistance can compensate for the undesirable effect of decrease in transmembrane pressure. The improvement (I) increases when the decrease in ring distance is rather rapid, as well as the value of a (the constant difference of an arithemetic series) increases, especially for higher feed concentration.

In addition to the effect of baffled-ring distance discussed in present study, the effect of baffled-ring number on the performance may have to be also taken into consideration. There may exist the proper baffled-ring number for properly adjusting the reduction of concentration polarization resistance while still preserving the effective transmembrane pressure, leading to further improved performance. The study with this equipment configuration by simultaneously adjusting the proper baffled-ring number and baffled-ring distances, will be our further work.

Symbols

A	—	constant defined by Eq. (11) (Pa)
a	—	Constant difference of a arithmetical series
B	—	constant defined by Eq. (12) (1/m)
C	—	constant defined by Eq. (15) (Pa)
C_i	—	Concentration of feed solution (wt.% dextran T500)
d_j	—	ring distance between (j – 1)th and jth rings (m)
$\bar{f}_1$	—	average overall friction factor
$\bar{f}_1, \bar{f}_2$	—	average friction factor on membrane and ring rod surfaces, respectively
J	—	permeate flux of solution (m^3/m^2 s)
$\bar{J}$	—	average value of J (m^3/m^2 s)
kr_m	—	radius of steel rod (m)
L	—	effective length of membrane tube (m)
P	—	pressure distribution on the tube side (Pa)
P_s	—	uniform permeate pressure on the shell side (Pa)
ΔP	—	transmembrane pressure, p-ps (Pa)
Q	—	volume flow rate in a tubular-membrane module (m^3/s)
r_m	—	inside radius of membrane tube (m)
R_f	—	resistance due to solute adsorption and fouling (Pa s/m)
R_m	—	intrinsic resistance of membrane (Pa s/m)
u_b	—	bulk fluid velocity in the flow channel (m/s)
z	—	axial co-ordinate, flow direction (m)
W	—	hydraulic dissipated power (N m/s)

Greek letters

ϕ	—	proportion constant (m^2s/m)
τ_1, τ_1	—	shear stresses on membrane and rod surfaces, respectively (Pa)

Subscripts

i	—	at the inlet
O	—	at the outlet

References

[1] S. Nokao, T. Nomura and S. Kimura, Characteristics of Macromolecular gel layer formed on ultrafiltration tubular membrane, AIChE J., 25 (1979) 615–622.
[2] M.J. Clifton, N. Abidine, P. Aptel and V. Sanchez, Growth of the polarization layer in ultrafiltration with hollow–fiber membranes, J. Membrane. Sci., 21 (1984) 233–246.
[3] D.C. Thomas, Enhancement of forced convection heat transfer coefficient using detached turbulence promoters, Ind. Eng. Chem. Process Des. Dev., 6 (1967) 385–390.
[4] S. Poyen, F. Quemeneur, and B. Bariou, Improvement of the flux of permeate in ultrafiltration by turbulence promoters, Int. Chem. Eng., 27 (1987) 441–447.
[5] A.R. Da Costa, A.G. Fane C.J.D. Fell, and A.C.M. Franker, Optimal channel spacer design for ultrafiltration, J. Membrane. Sci., 62 (1991) 275–291.
[6] J.A. Howell, R.W. Field, and Dengxi Wu, Yeast cell microfiltration: Flux enhancement in baffled and pulsatill flow system, J. Membrane. Sci., 80 (1993) 59–71.
[7] A.R. Da Costa, A.G. Fane and D.E. Wiley, Spacer charaterization and pressure drop modulling in Spacer-filled channels for ultrafiltration, J. Membrane. Sci., 87 (1994) 79–98.
[8] B.B. Gupta, J.A. Howell, D. Wu, and R.W. Field, A helical baffle for cross-flow microfiltration, J. Membrane. Sci., 99 (1995) 31–42.
[9] R.W. Field, D. Wu, J.A. Howell and B.B. Gupta, Critical flux concept for microfiltration fouling, J. Membrane. Sci., 100 (1995) 259–272.
[10] J.A. Howell, R.W. Field, and D. Wu, Ultrafiltration of high viscosity solution: Theoretical Developments and Experimental Findings, Chem. Eng. Sci., 51 (1996) 1405–1415.
[11] H.M. Yeh and H.H. Wu, Membrane ultrafiltration in combined hollow–fiber module systems, J. Membrane. Sci., 124 (1997) 93–105.
[12] H.M. Yeh and J.W. Tsai, Membrane ultrafiltration in multipass hollow–fiber modules, J. Membrane. Sci., 142 (1998) 61–73.
[13] H.M. Yeh, H.Y. Chen and K.T. Chen, Membrane ultrafiltration in a tubular module with a steel rod inserted concentrically for improved performance, J. Membrane. Sci., 168 (2000) 121–133.
[14] H.M. Yeh and K.T. Chen, Improvement of ultrafiltration performance in tubular membranes using a twisted wire-rod assembly, J. Membrane. Sci., 178 (2000) 43–53.
[15] B.H. Chiang and M. Cheryan, Ultrafiltration on skim milk in hollow fibers, J. Food. Sci., 51 (1986) 340–344.
[16] H.M. Yeh and Y.F. Chen, Momentum balance analysis of permeate flux for ultrafiltration in tubular membranes with gradually increasing incidental angles of a wired-rod insert, J. Membrane. Sci., 278 (2006) 205–211.
[17] C.C. Lin, Effect of ring distance on the performance in ring-rod tubular-membrane ultrafiltration, M.S. thesis, Tamkang University, Tamsui, Taiwan, 2006.